

## Results of JET Pellet Fuelling Experiments with Outboard and Inboard Launch

T.T.C. Jones<sup>3</sup>, L.R. Baylor<sup>1</sup>, C.D. Challis<sup>3</sup>, S.J. Cox<sup>3</sup>, C. Gormezano<sup>4</sup>,  
C.W. Gowers<sup>3</sup>, L.D. Horton<sup>5</sup>, P.T. Lang<sup>2</sup>, P.J. Lomas<sup>3</sup>, G.F. Matthews<sup>3</sup>,  
G. Saibene<sup>6</sup>, P. Twynam<sup>3</sup>, A.D. Walden<sup>3</sup>, M.J. Watson<sup>3</sup>, S. Wijetunge<sup>3</sup> and B.L. Willis<sup>3</sup>

*JET Joint Undertaking, Abingdon, Oxon. OX14 3EA, UK.*

<sup>1</sup>*Oak Ridge National Laboratory, Oak Ridge, TN, USA*

<sup>2</sup>*Max-Planck- Institut fur Plasmaphysik, Garching, Germany*

<sup>3</sup>*Euratom/UKAEA Fusion, Association, Culham Science Centre, Abingdon, UK*

<sup>4</sup>*Present address: Associazione Euratom/ENEA sulla fusione, Frascati, Italy*

<sup>5</sup>*Present address: Max-Planck- Institut fur Plasmaphysik, Garching, Germany*

<sup>6</sup>*Present address: EFDA CSU, Max-Planck- Institut fur Plasmaphysik, Garching, Germany*

### 1. Introduction

The JET pellet centrifuge and flight tube system were modified during 1999 to incorporate an in-vessel track to allow pellet launch from the inboard High Field Side (HFS) of the magnetic axis. The launch point is approximately on the midplane and the trajectory is tangential to the flux surface at normalised minor radius  $\approx 0.6$ . A fast-acting selector mechanism permits individual pellets or sequences to be diverted either to the inboard or outboard Low Field Side (LFS) tracks. The pellet extruder, cutter and centrifuge form and accelerate 4mm cubic pellets at speeds up to 500m/s (160m/s used in the present work) with a maximum design repetition rate of 10Hz. The object of the present experiments was to confirm whether or not the favourable effect of  $E \times B$  drift, shown to be beneficial for the fuelling effectiveness for HFS pellet injection in other devices [1,2], operates in JET plasmas and to establish any dependence on target plasma parameters. Results of preliminary experiments exploiting HFS pellets to re-fuel ELMy H-mode and ITB plasmas are also described briefly.

### 2. Physical Processes Controlling Pellet Deposition and Re-distribution

The net deposition of the pellet material in the target plasma is a combination of (i) the penetration distance  $\lambda_{\text{penetration}}$  of the ablating pellet and (ii) the plasmoid radial displacement distance  $\Delta$ . The sign of  $\Delta$  is the same for both inboard- and outboard- launch pellets, and this is the underlying reason for the expected difference in fuelling effectiveness of the two launch configurations, since the displacement is towards the magnetic axis for inboard-launch pellets, and away from the axis for outboard-launch pellets. The processes of ablation and  $E \times B$  drift are illustrated schematically in Fig.1. Any differences in fuelling characteristics and density profile response between otherwise similar discharges with inboard- and outboard- pellet launch should be attributable mostly to the  $E \times B$  drift effects. The dominant driving term is the pressure of the ablatant plasmoid, and so heating power and stored energy of the target plasma are expected to have

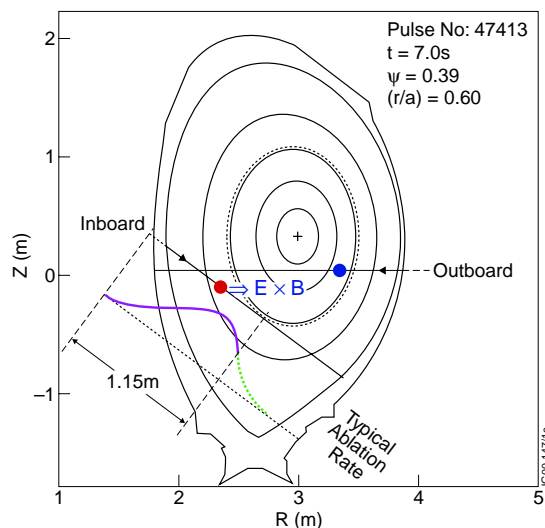


*Fig.1 Geometry of outboard and inboard-pellet launch trajectories in a typical JET plasma equilibrium. Typical ablation profile and schematic indication of  $E \times B$  drift beyond ablation zone are shown for inboard launch*

the most influence, with  $\Delta \propto \Delta\beta_{av} q^2 R$  where  $\Delta\beta_{av}$  is the spatial average enhancement of  $\beta$  resulting from fast re-heating of the plasmoid [3]. Since it is the electron thermal energy which is responsible for the fast re-heat of the plasmoid, and  $T_e$  which dictates mainly the pellet penetration distance, RF heating was mostly used and varied between about 2MW and 7.5MW in the present investigation. The expression for  $\Delta$  also implies a possible dependence on  $q$  (and magnetic field through  $\beta$ ) therefore limited scans of  $I_p$  and  $B_T$  were also carried out. L-mode target plasmas were employed, having good reproducibility, particularly for RF heating, and the vertical  $D_{alpha}$  measurements could be used to give an indication of ablation rate (from the light intensity) since the background  $D_{alpha}$  intensity is low in L-mode and there are no ELMs.

### 3. Comparison of Prompt Density Profile Response with Ablation Profile

Figures 2, 3(a) and 3(b) show the change  $\Delta n_e(\rho)$  in density profile (from LIDAR measurements) for outboard and two inboard pellet injection cases respectively, for the target plasma parameters indicated. Figure 2 shows the computed particles deposited per unit volume according to the Neutral Gas Shielding (NGS) model [4] calculation [on the same scale as  $\Delta n_e(\rho)$ ], where the radial co-ordinate  $\rho$  is the square-root of the poloidal flux function. Figures 3(a) and 3(b) (inboard-launch) show the  $D_{alpha}$  ablation light, measured as a function of time and mapped onto the co-ordinate  $\rho$  using the known pellet injection velocity (assumed constant) and trajectory. In the data of Fig.2 (outboard-launch) there is no significant increase of density beyond the zone of ablation, as computed by the NGS code. Of course, none would be expected from the initial deposition of pellet mass since the  $E \times B$  drift effect would carry ablatant away from the core. There is, however, the possibility that particle transport might cause diffusive flow of the resultant plasma particles towards the core but this effect is evidently not significant on the timescale (30ms) involved here. In Figs. 3(a) and (b) (inboard-launch), however, there is significant accumulation of particles within the core region. Whilst the NGS code prediction has its limitations, a feature of the particular JET inboard-launch geometry is that the trajectory becomes tangential to the flux-surface at about  $\rho = 0.7$ . Therefore a ‘‘cut-off’’ in ablation at this radius is a necessary geometric consequence and is not dependent on the details of modelling. The  $D_{alpha}$  trace is plotted in two colours; corresponding to the ‘‘first-pass’’ of the pellet up to the tangency point, and thereafter corresponding to the pellet’s ‘‘second-pass’’. Figures.3(a) and 3(b) compare data for inboard-launch pellets at two power levels, 2.6MW and 7.2MW respectively. The pellet ‘‘overshoots’’ the tangency radius, and at high power the ablation stops short of this point. Consequently, in both cases, the pellet ablation and initial deposition are peripheral, yet the LIDAR density profile response clearly indicates core fuelling in a region where direct ablation does not occur.

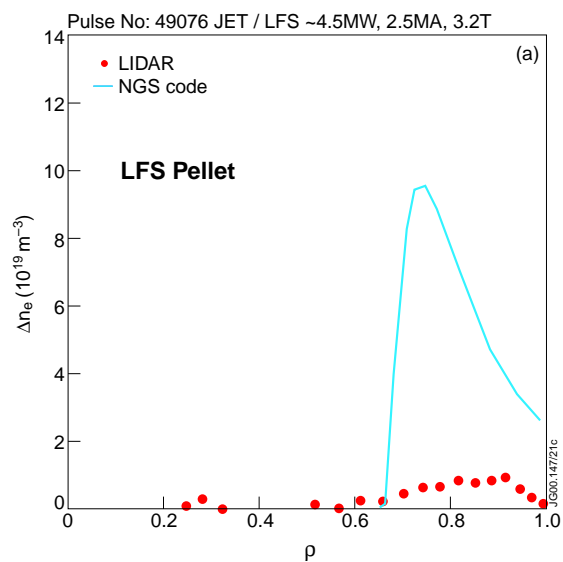


Fig.2 Comparison of density profile change with ablation profile, computed from NGS code. Outboard (or Low Field Side (LFS)) launch

### 4. Dependence of Core Fuelling Characteristics on Plasma Target Parameters

The inboard-launch results suggest a dominant role from  $E \times B$  drift effects, and it is of particular interest to investigate how this might vary with target plasma parameters and whether any of the expected physical dependences might be exhibited. An indication of possible  $E \times B$  drift is assumed to be the increase in particle content in the core region of the plasma beyond the ablation zone, taken to be  $\rho < 0.7$ . If the time interval between pellet entry and the LIDAR density profile measurement is

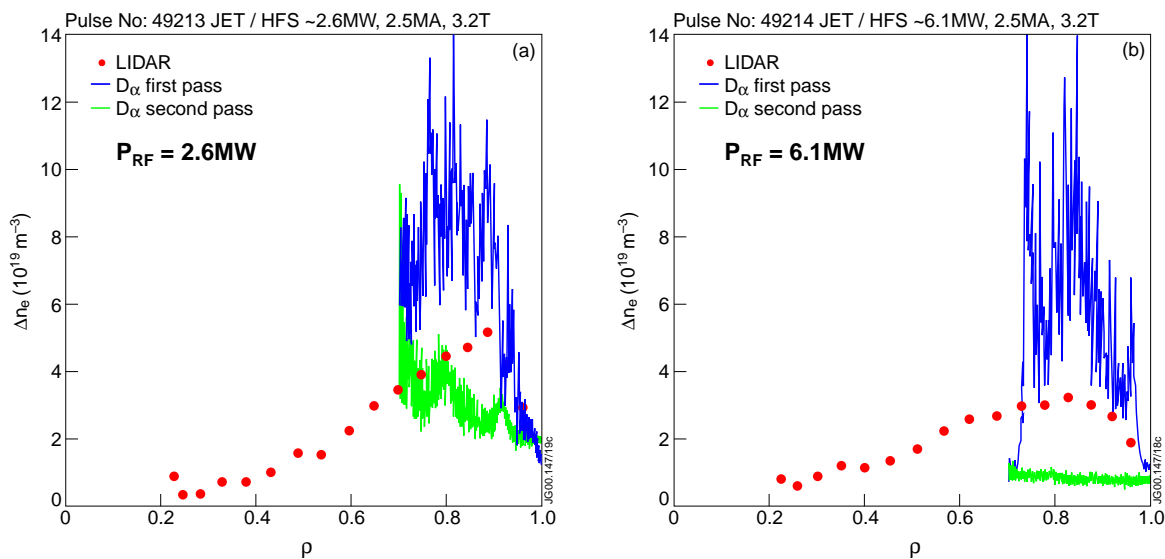


Fig.3 Comparison of density profile change (45ms after pellet entry), also showing  $D_{\alpha}$  ablation light (assumed proportional to ablation rate) mapped to flux-surface co-ordinate for Inboard (or High Field Side (HFS)) launch. a) Low power L-mode, b) High power L-mode

greater than several 10s of milliseconds the diffusive flow set up by the density gradient causes the profile to relax and also results in significant global particle exhaust, complicating the interpretation. The latter effect has been partly compensated for by expressing the change in particle content in the region  $\rho < 0.7$  as a fraction of the total particle content change accounted for in the entire plasma volume (though this increases the error bars deriving from the LIDAR data). In this way, variation in global particle exhaust due to different time delays and to changes in particle transport coefficients at different additional heating power, plasma current and toroidal field employed in the scan are taken into account. There is clear evidence that inboard-launch core fuelling effectiveness is maintained with increasing power (Fig.4(a)), and an improving trend cannot be discounted especially when plotted versus average electron pressure (Fig. 4(b)). This observation is consistent with the fact that the electron thermal energy represents the heat available to produce the ablatant  $\beta$  excursion ( $\Delta\beta_{av}$ ), the main driving term for  $E \times B$  drift. No significant trend could be established, from the available data, on the influence of magnetic field and  $q$ .

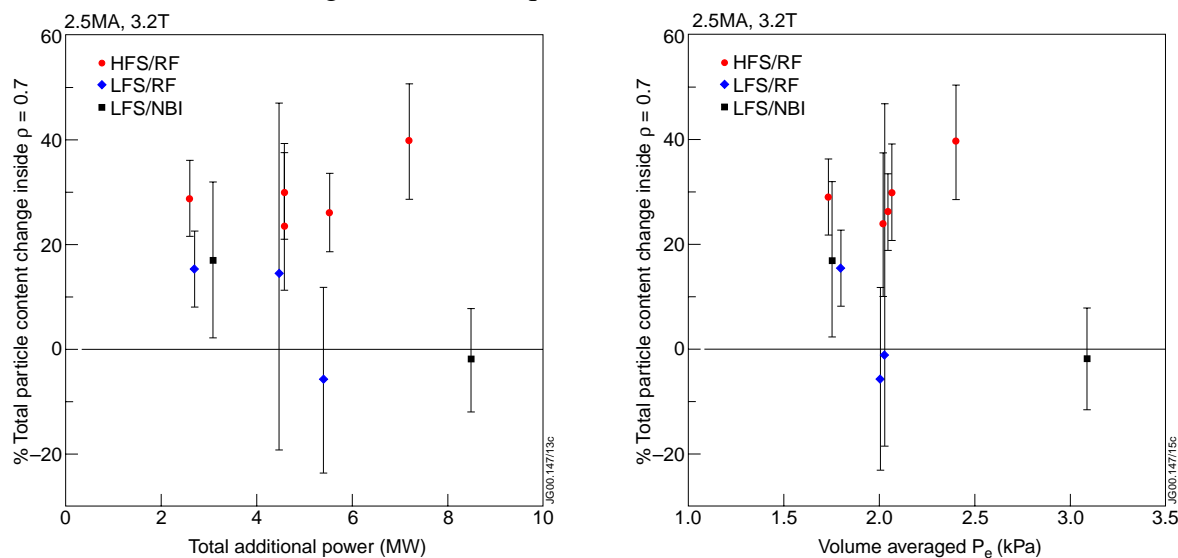


Fig.4 Percentage change of total plasma particle content from pellet injection accounted for beyond ablation zone ( $p < 0.7$ ). a) versus plasma heating power, b) versus volume average electron pressure

## 5. Inboard-launch pellet re-fuelling of H-mode and ITB plasmas

Figure 5 shows that H-mode re-fuelling by inboard-launch pellets is remarkably effective, in contrast to outboard-launch. There is, however, some loss of energy confinement, in similar fashion to gas fuelling, but at higher values of average density which can exceed the Greenwald limit. The confinement reduction is attributed to the low temperatures produced and degradation of NB heating profile. By reducing the pellet size and optimising the delivery sequence the density rise is lower (90% Greenwald limit) but with only moderate reduction in temperature and loss of stored energy ( $\approx 10\%$ ) [5]. Inboard pellets are also effective in re-fuelling a pre-existing ITB barrier, but so far this has not been achieved without causing a temporary destruction of the confinement barrier, though it can re-form before the density has completely decayed (Fig. 6).

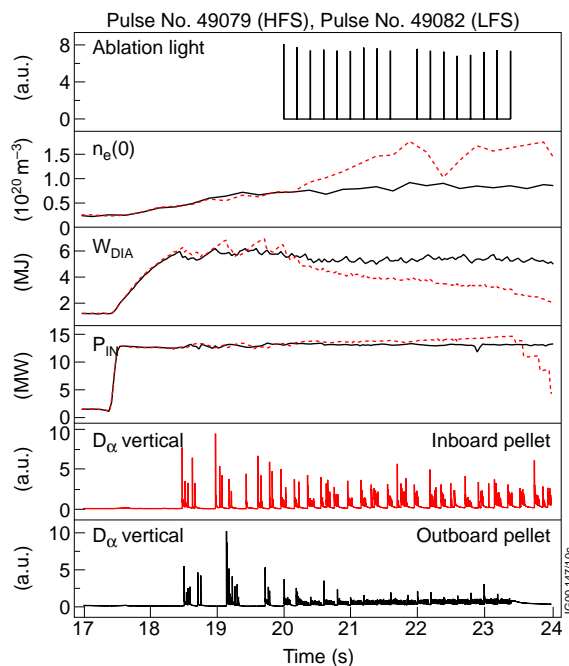


Fig.5 Comparison of outboard (LFS) and inboard (HFS) pellet fuelling of ELMy H-mode plasmas

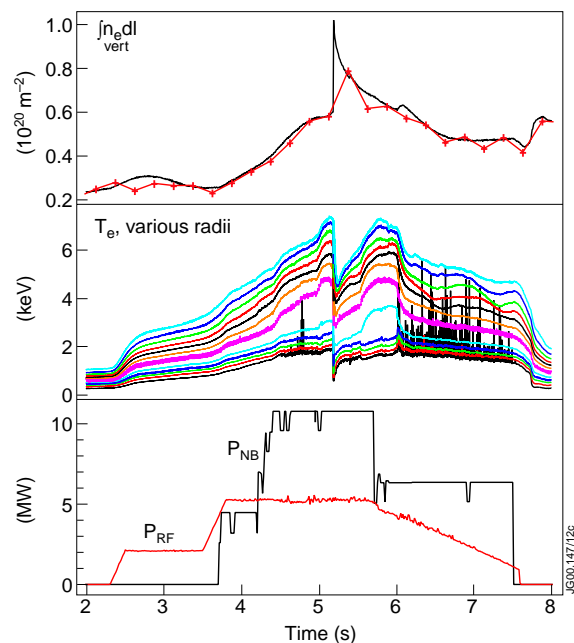


Fig.6 Inboard (HFS) pellet re-fuelling of ITB Plasma

## 6. Conclusion

The principal result derived from the present experiments is that inboard-launch pellets exhibit superior core fuelling characteristics over a range of plasma conditions with strong auxiliary heating, including enhanced confinement modes. This is not an unexpected result, based on the present physical understanding of the underlying processes in which the cold plasmoid  $\beta$  enhancement is the main driving term for E $\times$ B drift. Nevertheless, the net fuelling effectiveness is a competition between ablation and drift effects and it was important to demonstrate in JET-sized plasmas that the favourable characteristics are still maintained.

## References

- [1] P T Lang et al., Phys Rev Lett **79** 8 (1997) 1487
- [2] L R Baylor, et al. Physics of Plasmas **7** 5 (2000) 1878
- [3] H W Müller et al., Phys Rev Lett **83** 11 (1999) 2199
- [4] L R Baylor, A Géraud et al., Nucl Fusion **37** (1997) 445
- [5] P T Lang et al., Contributed Paper, these Proceedings